Co-published by
Institute of Fluid-Flow Machinery
Polish Academy of Sciences
Committee on Thermodynamics and Combustion
Polish Academy of Sciences

http://www.imp.gda.pl/archives-of-thermodynamics/

Gibbs-Duhem equation used to describe uncompensated and apparent heat transfer applied to spray cooling

Stephanie Lacour[a*], Michel Feidt[b]

[a]Université Paris-Saclay, INRAE - Unite de recherche FRISE, Pierre-Gilles de Gennes 1, CS 10030, Antony 92761, Cedex, France
[b]University of Lorraine, Laboratory LEMTA, 2 Av. de la Forêt de Haye, 54500 Vandœuvre-lès-Nancy, France
*Corresponding author email: stephanie.lacour@inrae.fr

Received: 06.12.2024; revised: 25.03.2025; accepted: 06.04.2025

Abstract

Entropic analysis makes it possible to determine the equilibrium of a system with its environment, but heat exchange at boundaries is a difficulty in this exercise. In this article, we establish the energy balance of a water liquid and air mixture: the Gibbs-Duhem equation is used to describe the balance. Diffusion terms are expressed while accounting for volume changes and their entropic contributions, leading to an expression for fugacity. After mixing, the mixture spontaneously evolves combining mechanical, chemical and thermal changes towards equilibrium. This latest is solved assuming either an isenthalpic or isentropic transformation in the balance, to highlight the energy exchange between the system and its environment. Some irreversibilities are included in transformations and primarily affect the chemical path. The comparison reveals heat transfer terms corresponding to uncompensated heat. This analysis illustrates the concept of uncompensated heat and introduces its complement, the apparent heat, which corresponds to enthalpy. The models explain the limiting phenomena involved in spray cooling, whose efficiency varies depending on whether the process follows an adiabatic or an isenthalpic path. The isenthalpic model was applied to literature data to estimate experimental cooling efficiencies over a wide range of operating conditions. However, further modelling work is needed to express the scaling factor for fugacity as a function of the droplet size distribution. The mechanical pathway also requires more attention and dedicated measurements are needed to include pressure drops in the analysis.

Keywords: Gibbs-Duhem equilibrium; Uncompensated heat transfer; Irreversibility analysis; Misting process; Evaporating cooling

Vol. 46(2025), No. 2, 209–219; doi: 10.24425/ather.2025.154919

Cite this manuscript as: Lacour, S., & Feidt, M. (2025). Gibbs-Duhem equation used to describe uncompensated and apparent heat transfer applied to spray cooling. *Archives of Thermodynamics*, 46(2), 209–219.

1. Introduction

Spray cooling of air, heat exchangers or electronic devices allows adapting heat-releasing systems to our actual atmosphere, overheated by climate change. Many studies were carried on to describe the spray cooling efficiencies and their related operating parameters in various evaporative applications: for a direct use outdoors [1], in direct heating, ventilation, and air conditioning (HVAC) systems [2−7], in indirect or M-cycle air coolers [8−11], for heat releases in chillers [12−15] or cooling towers [16−21], or electronic applications [22,23]. Most of the time, results are given according to a simplified thermal analysis: efficiency is found by comparing results to the guess state, which is the saturated state of air. Because of the spontaneous and uncontrolled nature of evaporation, attention is not paid to the physical processes that alleviate efficiency. The complete evaporation of a spray is rarely observed in experimental studies reported in the literature [1,3,6]. Actual development in spray cooling techniques relies on intermittent injection, in order to save water and

Nomenclature

C_p – molar heat capacity, J mol^{-1} K^{-1}
d – droplet diameter, m
H – enthalpy, J
HR – relative humidity, %
H_{vap} – enthalpy for water phase change, J mol^{-1}
k – scaling factor
M – mass of compound, kg
$\tilde{M}$ – molar mass, kg/mol
n – mole of compound, mol
N – number of droplets, m^{-3}
P – pressure, Pa
R – ideal gas constant, J mol^{-1} K^{-1}
S – entropy, J K^{-1}
S_d – entropy for partial pressure change, J K^{-1}
S_v – entropy for volume change, J K^{-1}
S_{vap} – entropy for water phase change, J mol^{-1} K^{-1}
T – temperature, K
V – volume, m^3
x – evaporated mole of water, mol

Greek symbols

α – exponent in the scaling factor
β_i – coefficient in the evaporation temperature relation
γ – adiabatic index
ρ – phase density, kg m^{-3}
μ_i – chemical potential of water in phase i, J mol^{-1}
δQ – heat exchange, J
δW – work exchange, J

Subscripts and Superscripts

d – droplet
eq – equilibrium
f – final state
g – gas
i – initial state
l – liquid
v – water vapour
vap – vaporisation
m – initial mix (liquid+gas)
t – total of compounds
x – related to vapour at the early stage of evaporation
0 – standard state

let the system dry out regularly [24]. Nevertheless, spray cooling techniques would surely be improved if more care was paid to the exceeding liquid water, remaining as a result of non-ideal, not the so-called adiabatic, cooling. Hence, irreversibilities have to be studied, which can be done using entropy analysis.

Entropic analysis in classical thermodynamics allows the study of the irreversibilities of a system that undergoes transformations. Advances in thermodynamics of finite physical dimensions integrate these irreversibilities into methods of optimizing energy systems [24]. Entropy is often used for spray in order to predict the size of spray droplets using the maximum entropy formalism [26]. Le Moyne et al. in [27] explored the concept of scale entropy, shifting from the self-similarity theory to the so-called 'close-to-fractal' evolution to describe spray atomization. Such mechanistic approaches are less suited when dealing with evaporative cooling because the focus is mainly on the thermal change, not addressed in mechanics. Combined heat and mass transfer phenomena are also usual problems handled with thermodynamics. Water in moist air is one of the well-documented ones [25,28]. The entropy of moist air was studied in atmospheric problems. Dynamic and thermal pathways were examined to assess the entropy production in the Earth's atmosphere and study the piston effect of convection with moist air [29]. The chemical pathway is added to describe convective motion in cloud formation [30]. In the latest, local entropy deficits explain convective air entrainment and cloud size evolution. Piston effect in spray and moist air was even exploited for an evaporative engine in [31]. For an evaporative cooler, the entropy analysis is a basis for exergy assessments [28,32,33]. Most of the key psychrometrics processes used in HVACR (heating, ventilating, air conditioning and refrigeration) were studied by Ratlamwala and Dincer [33], using various definitions for energy and exergy efficiencies. For an evaporative cooler, they considered a complete evaporation of the liquid water in the process. Energy efficiencies were, however, highly different according to the benefits brought by such an ideal process and its related efficiency definition. In the work of Santos and Barros [34], the second law gives an interesting insight for assessing the exergy efficiency of air washers. In the same way, entropy analysis was successfully used by Wang et al. [35] for the optimization of a M-cycle cooler. Smekar et al. in [16] also used the entropy approach to link local temperature fluctuations and their related entropy to the efficiency of a cooling tower. Majunath et al. [36] used the second law of thermodynamics in a heat exchanger to reduce irreversibilities with an optimal design. Like in [34] or [35], the entropy generation is used for quantifying irreversibilities. However, in an adiabatic cooling method, such as spray cooling, both entropy generation and entropy transfer are critical factors that influence cooling efficiency. The transformation during spray cooling involves multiple pathways related to chemical, thermal and mechanical changes. Therefore, it is essential to integrate these pathways into a comprehensive energy analysis of the system.

Defining a system consists of delimiting a portion of the Universe, whose behaviour is described in detail and which is opposed to the rest, that is, "its environment". The existence of the system is thus based on the notion of the geometric dimensions assigned to the system by defining it. The transfer of mass and energy at the boundary is generally described, but that of entropy at the boundary is rarely addressed. Bejan [28] evokes the difficulty associated with accounting for these transfers in his work. He underlines the problem of boundaries of isolated systems, which are often subjected to temperature gradients.

The isolated system is a limit case, with no transfer of mass or energy to the environment. The absence of transfer simplifies

the description of system transformations, making it ideal. The actual state observed generally differs from the ideal state: this is then attributed either to imperfections in the insulation of the system (transfers), or to irreversibilities (internal productions) which prevent a return to the initial state. The distinction between irreversibility and transfer is delicate: the two terms, generally second-order, are often confused. In open systems, energy transfer at the boundaries occurs, internal irreversibilities are present and are easily confused with the irreversibilities of transfers. Exchange at the boundaries also includes the transfer of matter, but the latter does not better explain the distinction between entropic and thermal transfer at the boundaries. The purpose of this paper is to highlight the distinction between transfer terms and internal irreversibilities in spray cooling. Therefore, we study the spontaneous evolution of a mixture of air and liquid water in free conditions. Mixing generates an imbalance, which causes the two phases to evolve towards a state of equilibrium. In the Lagrangian approach, the mixture evolves spatially in a tunnel at the entrance of which we carry out the mixing, and at the exit of which we recover a mixture assumed to be in equilibrium: we describe an open system in a permanent steady state. In the Eulerian approach, the description involves the temporal evolution of the mixture in a spatially limited closed space, which exchanges energy at its boundaries. A succession of transformations details the chemical, thermal and mechanical processes at work in the evolution of the mixture. The Gibbs-Duhem equation, extended to this non-isolated system, brings together these three types of thermal, mechanical and chemical processes in a global equation of evolution. The equilibrium is expressed with an assumption regarding chemical equilibrium and two alternatives for the thermal equilibrium. The internal irreversibilities for this system control the position of the chemical equilibrium, while the heat transfer terms are of small amplitudes. Entropic transfers systematically differ from thermal transfers and analytically explain the notion of uncompensated heat.

2. Materials and methods

2.1. Mixing moist air with liquid water

Mixing operation induces a temporary non-equilibrium state in the system's components, enabling the extraction of a useful effect such as cooling during the relaxation back to equilibrium. Mixing is often used to quicker obtain an equilibrium state, adding convection transport to diffusion processes. Optimization serves to minimize the cost of creating an imbalance state, while maximizing the service provided. This approach is not the subject of our description and we are not interested here in the energy cost of unbalancing. On the other hand, we use entropic analysis to identify the parameters that impose the final position of the equilibrium. Indeed, these parameters describe the accessible final state. We use a method based on the control volume approach [37] to describe the evolution of the energy terms corresponding to the movement towards equilibrium of our mixture.

Entropy analysis allows identify the intrinsic physical limitations of our mixture. Just as Chambadal and Curzon-Alborn [38] demonstrated that Carnot's efficiency was inaccessible due to the need to have a temperature gradient to carry out heat transfer, we seek here to express the effective cooling obtained from the mixture of air and water. Entropy analysis is one way to achieve this. We apply it here to operating mixing conditions, given a quantity of humid air at a known temperature and humidity (T, M_g, HR) and a quantity of liquid water (M_l, T_w = T). In a stationary or permanent dynamic regime, (M_g) and (M_l) will be quantities per unit of time, while they will be the extensive quantities in the Eulerian approach. Such a mixture of humid air and water is a classic thermodynamic system. Many authors have shown that the evolution of these mixtures involves a path of transformations, which combines thermal, mechanical and chemical modifications [32,39]. Most of the time, particularly in exergy approaches [36], the final state is assumed to correspond to the adiabatic saturation state of the air. Adiabatic saturation is related to the reference state, assuming infinite air volumes. In a finite volume, the final equilibrium state differs from adiabatic saturation. To describe the effective cooling, a succession of transformations makes it possible to express the mechanical, thermal and chemical contributions. These are detailed in the following paragraph. Physical processes are broken down to simply express transformation terms.

2.2. Path of transformations

2.2.1. Evaporation stage

A quantity of water (x) is transformed into vapour and this physicochemical transformation modifies enthalpy, entropy and chemical potential by modification of the reference values. For enthalpy, the reference values are preferred to its definition with internal and PV energies (where PV energy arises from the pressure (P) and volume (V) of fluid): enthalpy is more likely used in this form in evaporative cooling. Thus, we have:

$$dH = (H_g^0 - H_l^0)dx = H_{vap}dx, \quad (1)$$

$$dS = (S_g^0 - S_l^0)dx = S_{vap}dx, \quad (2)$$

$$d\mu = (H_{vap} - TS_{vap})dx. \quad (3)$$

2.2.2. Vapour diffusion stage

Water in the vapour state occupies a volume V_x greater than the volume occupied in the liquid state. This volume of gas diffuses into the total volume of air V_g and generates entropy. This contribution is obtained by writing the variation in volume entropy, between the initial state V_i and the final volume V_f, for each component j of the gas mixture containing n_g moles of air, and by deriving with respect to the evaporated quantity dx:

$$S_v = R\sum_j n_j \ln\frac{V_{jf}}{V_{ji}} = R\left(n_g \ln\frac{V_{gf}}{V_{gi}} + x\ln\frac{V_{xf}}{V_{xi}} + n_l \ln\frac{V_{lf}}{V_{li}}\right).$$

Neglecting the volume variation for the liquid content and assuming that water evaporates at a constant atmospheric pressure, one obtains

$$S_v = R\left(n_g \ln\frac{n_g+x}{n_g} + x\ln\frac{n_g+x}{x}\right) \Rightarrow dS_v = -R\ln\frac{x}{n_g+x}dx. \quad (4)$$

This term corresponds to the diffusion of vapour in the gas volume. At constant pressure and temperature, it represents the non-ideality resulting from the gas volume and molar increase associated with the phase change. Due to its form, this term is assumed to balance the fugacity required for a non-ideal reaction. The homogenization of the partial pressures of water vapour and liquid water is also accounted for by expressing the diffusion entropy according to the mixing law, known as Amagat's diffusion. The Amagat's diffusion is also balanced with partial pressure terms in the chemical potential.

2.2.3. Compression stage

Our diffusion model does not keep the volume. Hence, a compression step is added to keep an isochoric evolution. The gas volume ($V_g + V_x$) is compressed to retrieve the initial volume V_g through an isentropic compression following:

$$PV^{\gamma} = \text{const.} \tag{5}$$

Temperature, pressure and volume are modified and affect all three paths. Although the mix composition does not vary during this step, all changes are related to the evaporated quantity, which determines the initial volume of this step. For an ideal gas, we get

$$PdV = -\gamma RT_m \left(\frac{n_g+x}{n_g}\right)^{\gamma} dx, \tag{6}$$

from which the pressure drop and thermal changes are established, where T_m is the initial mixing temperature, used here to alleviate notations.

2.2.4. Cooling stage

The energy required to convert dx moles of water from liquid to vapour produces a significant decrease in thermal energy, which results in a decrease in the temperature of a mixture and a pressure drop. The pressure change modifies the chemical potential:

$$dH = n_t C_{p,m} dT, \tag{7}$$

$$VdP = n_g R dT, \tag{8}$$

$$(\mu_g - \mu_l)dx = RT \ln \frac{P_f}{P_i} dx. \tag{9}$$

2.3. Gibbs-Duhem equation

The Gibbs-Duhem equation brings together the different contributions of the thermal (dH), mechanical (VdP) and chemical ($(\mu_g - \mu_l)dx$) pathways, revolving around the evolution of entropy, written in the form

$$dH = VdP + (\mu_g - \mu_l)dx + TdS. \tag{10}$$

This equation makes it possible to track the energy redistributions, which take place as the transformations progress. The order of the transformations does not matter. All the terms detailed before are reported in Table 1 and brought together in Eq. (10) by equating all terms of the first column to all those of the second, third and fourth columns.

Any modification of the thermal state (dH) has repercussions on the entropy. Similarly, the chemical and mechanical states also contribute to the entropy term TdS. In all the transformations, the Gibbs-Duhem energy terms are balanced. The exhaustive writing of the terms makes it possible to analyse the energy redistributions from one path to another, as shown in Fig. 1.

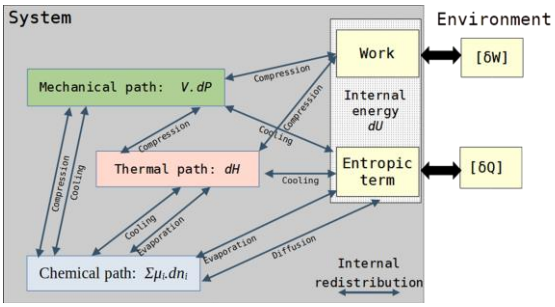

Fig. 1. Energy variation of control volume in its evolution towards a state of equilibrium: storage in internal energy, energy redistributions and exchange with the environment.

Table 1. Decomposition of energy terms in Gibbs-Duhem equation corresponding to dx moles of liquid water, which evaporates at a constant volume (see text for the stage description).

	Thermal path	Mechanical path	Chemical path	δQ	$-\delta W$
Operation	$dH =$	$VdP +$	$(\mu_g - \mu_l)dx$	$+ TdS$	
Evaporation	$H_{vap}dx$		$(H_{vap} - TS_{vap})dx$	$TS_{vap}dx$	
Mixing S_v S_d	0	0	$RT \ln\left(\frac{x}{n_g+x}\right)dx$ $RT \ln\left(\frac{n_v+x}{n_l-x}\right)dx$	$-RT \ln\left(\frac{x}{n_g+x}\right)dx$ $-RT \ln\left(\frac{n_v+x}{n_l-x}\right)dx$	$RT_m dx$
Compression	$\gamma RT_m \left(\frac{x}{n_g+x}\right)^{\gamma} dx$	$\gamma RT_m \left(\frac{x}{n_g+x}\right)^{\gamma} dx$	$RT \ln\left(\frac{n_g+x}{n_g}\right)^{\gamma} dx$	$-RT \ln\left(\frac{n_g+x}{n_g}\right)^{\gamma} dx$	$-RT_m \left(\frac{x}{n_g+x}\right)^{\gamma} dx$
Cooling	$n_t C_{p,m} dT$	$n_g R dT$	$RT \ln\left[\frac{T}{T_m}\left(\frac{n_g+x}{n_g}\right)^{1-\gamma}\right] dx$	$(n_t C_{p,m} - n_g \mathrm{R})dT$ $-RT \ln\left[\frac{T}{T_m}\left(\frac{n_g+x}{n_g}\right)^{1-\gamma}\right] dx$	

Likewise, the term TdS_d corresponds to the balancing of partial pressures. It was identified by Amagat as a diffusion entropy, which reflects the irreversibility of mixing. In our proposal, we brought out dS_v, the variation in entropy associated with the change in volume: this term balances with the fugacity in the chemical potential. The pressure drop recovers mechanical dissipation, marking the irreversibility of cooling. The whole entropic term TdS therefore contains dissipations, related to diffusion and mechanical degradations. It is not in exact correspondence with the thermal term dH, in the sense of [35]: the first describes the thermal energy transfer with the environment, while the second characterizes conversion processes that modify the thermal state of the system.

The entropic term governs heat exchange with the environment. In this, it is difficult to assess the reversible or irreversible nature of the subterms. Many terms are associated with the reduction of chemical potential and pressure. Others correspond to the thermal change in enthalpy and the change in the entropy of formation.

3. Results and discussion

3.1. Chemical potential of moist air with liquid water

Evaporation is driven by the chemical potential. The chemical potential, in exergy approaches concerning moist air, is expressed with the change of state term ($H_{vap} - TS_{vap}$) and the partial pressure equilibrium (S_d). For pure water, the potential is positive at ambient temperature and becomes negative at 100°C. Spontaneous evaporation is not possible. Mixed with ambient air, the chemical potential is set to zero at adiabatic saturation conditions for the air; it is the reference state − or dead − state used in exergy approaches [28]. In the present work, the entropy of volume change was used to express the fugacity without using a reference state.

Thus, the chemical potential is completely defined and evolves during evaporation: very negative at start, it increases with the quantity of water evaporated, as can be observed in Fig. 2. The spontaneous evaporation ends when the chemical potential becomes positive. At zero, an equilibrium is found and the evaporation is stopped. This occurs before saturation, because the contribution of fugacity (S_v) is larger than the constant related to saturation conditions.

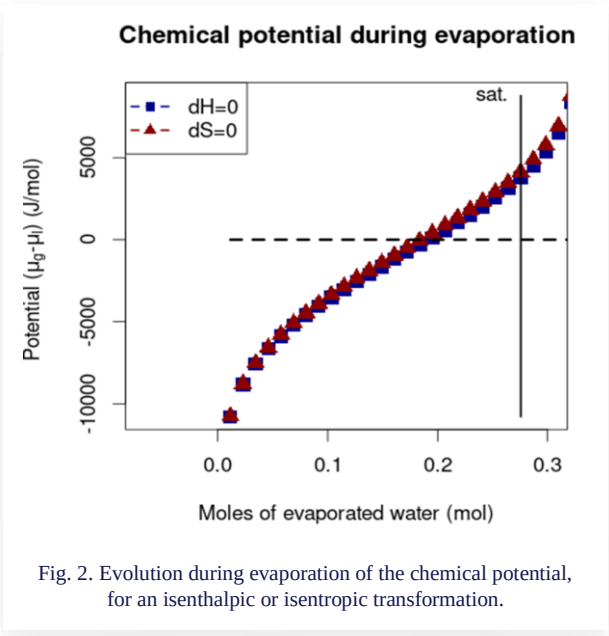

Fig. 2. Evolution during evaporation of the chemical potential, for an isenthalpic or isentropic transformation.

The vapour diffusion term (S_v, entropy of volume change, in red in Fig. 3) compensates for the positive terms. It is enough for a water molecule to break away from the liquid phase and pass into the much larger volume of gas; the number of possible positions (probable state) of this molecule is very large. This is the meaning of the entropy of volume change in a probabilistic approach (statistical mechanics). This entropy, very important at the start of the reaction, reduces as the number of vapour molecules increases. Hence, the diffusion of vapour initiates and controls the evaporation. As the liquid was neglected, this model

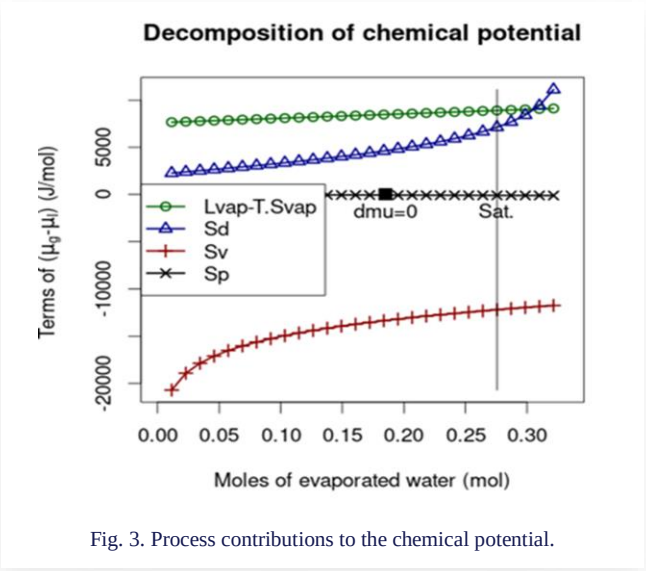

Fig. 3. Process contributions to the chemical potential.

applies only to a disperse spray mixture but gives, at $\Delta\mu = 0$, an estimate for the cooling efficiency of a mixture for the given operating conditions inside a finite volume.

3.2. Towards the equilibrium state

The evaporation of liquid water in air is a spontaneous reaction requiring a negative chemical potential. Also, setting the chemical potential to zero (the third column of Table 1 equals zero) is the condition for ending spontaneous evaporation and defining the chemical equilibrium. The cancellation of the chemical potential does not involve dx, nor dT, and is written as

$$0 = H_{vap} - TS_{vap} + RT \ln\left(\frac{n_v+x}{n_l-x}\frac{x}{n_g}\frac{T}{T_m}\right). \qquad (11)$$

Furthermore, cooling by evaporation of water in air is generally called adiabatic, which provides a second boundary condition. Classically, the overall process is assumed to be isenthalpic with $dH = 0$. The temperature gradient is then written as a function of the quantity of water evaporated, by making a series expansion of the exponent term (γ), which gives for the isenthalpic case:

$$dT = -dx\left(\frac{H_{vap}+\gamma RT_m}{n_t C_{p,m}} + x\frac{\gamma^2 RT_m}{n_g n_t C_{p,m}}\right). \quad (12)$$

Integrating gives:

$$T = T_m - \beta_1 x - \beta_2 \frac{x^2}{2} \quad (13)$$

with $\beta_1 = \frac{H_{vap}+\gamma RT_m}{n_t C_{p,m}}$ and $\beta_2 = \frac{\gamma^2 RT_m}{n_g n_t C_{p,m}}$.

The adiabatic system is without heat exchange with the outside, meaning that the entropic term is cancelled, $TdS = 0$. There, entropy reaches an extremum. As the production of entropy in the system can only be positive or zero, the isentropic equilibrium position corresponds to a minimum of entropy. By making the chemical equilibrium match with the minimum entropy, Eq. (11) is introduced into the entropic term to express the temperature gradient as a function of the quantity of evaporated water:

$$dT = -dx\left(\frac{H_{vap}}{n_t C_{p,m} - Rn_g}\right). \quad (14)$$

After integration, it yields:

$$T = T_m - \beta_1 x \quad \text{with} \quad \beta_1 = \frac{H_{vap}}{n_t C_{p,m} - Rn_g}. \quad (15)$$

Introducing this latest expression of $T(x)$ into the isentropic equation $dS = 0$ gives the expression for the chemical equilibrium at the minimum entropy:

$$0 = H_{vap} - (T_m - \beta_1 x)S_{vap} + \\ + R(T_m - \beta_1 x)\ln\left(\frac{n_v+x}{n_l-x}\frac{x}{n_g}\frac{T_m-\beta_1 x}{T_m}\right). \quad (16)$$

3.3. Comparing isenthalpic and isentropic solutions

The root of Eq. (16), namely, the isentropic solution, is assessed using an equation solver between 0 and n_l, the molar quantity of injected liquid water. The same procedure is applied to the isenthalpic case, combining Eqs. (11) and (13) (results are written later, in Eq. (18)).

Differences between the isenthalpic and isentropic approaches are illustrated for the following given operating conditions:

M_g = 1145 g, $T_g = T_l$ = 33°C, M_l = 6 g, HR = 40%.

Solutions are given in Table 2 for both cases. Chemical equilibrium is reached before evaporating all the injected liquid water in both cases.

The isentropic line, corresponding to Eq. (14), is represented in red in Fig. 4 and the blue line corresponds to the isenthalpic– Eq. (12). These curves represent the isentropic and isenthalpic evolution of temperatures with the evaporation. The equilibrium points are represented with the marks. In both cases, the final equilibrium state has a temperature above and a humidity below the adiabatic saturation point. Isentropic cooling, i.e. without heat exchange with the environment, provides access to a lower equilibrium temperature and ensures better cooling by evaporating less water. In the isenthalpic case, the surrounding environment transfers heat to the mixture: equilibrium temperatures are higher and water consumption is slightly higher than in the isentropic case. To increase cooling, the quantity of liquid water injected can be increased, as shown in [40].

Table 2. Temperature and evaporated liquid mass at chemical equilibrium of mixture for two cases.

Case	Equilibrium temperature (°C)	Evaporated mass (g)
Isenthalpic	25.3	3.5
Isentropic	23.6	3.3

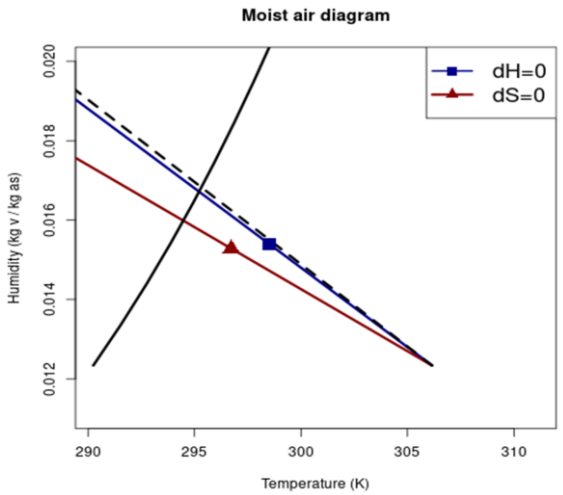

Fig. 4. Temperatures and quantities of liquid evaporated at equilibrium, assuming isenthalpic or isentropic transformation. Marks represent the equilibrium positions, the black curve is the saturation curve and the dotted black one is the air isenthalp curve.

3.4. Exchange with the environment

In the isentropic case, there is no heat exchange with the surrounding environment. It is the ideal case, where cooling is maximum. The real case, closer to the isenthalpic model, is not adiabatic, because $dS_{eq} > 0$ (dS_{eq} = 32 J/K, in the previous conditions). Heat ($\delta Q = TdS$) is transferred from the hot surrounding environment to the cooled system: the entropy of the system increases despite the drop in temperature. Inserting the isentropic equation (Eq. (14)) into the TdS term gives the following equation, where redistributions are identified:

$$\delta Q = TdS = dx\begin{bmatrix}(T_m - \beta_1 x)S_{vap} \\ + R(T_m - \beta_1 x)\ln\left(\frac{T_m-\beta_1 x}{T_m}\frac{x}{n_g}\frac{n_v+x}{n_l-x}\right) \\ +Rn_g\beta_1 \\ -n_t C_{p,m}\beta_1\end{bmatrix} \quad \begin{matrix} TdS\ [\text{formation}] \\ TdS[\mu] \\ TdS\ [P] \\ TdS\ [H]\end{matrix} \quad (17)$$

Entropic terms resulting from energy redistributions, via chemical, mechanical and thermal pathways, are identified according to the following methods: the thermal path is balanced with terms in the first column, the mechanical path with terms in the second column and the chemical path with terms in the third column. This latest includes only the diffusion process and the phase change was separated. Entropic contributions are quantified at equilibrium for the previous test conditions and compared for the isentropic and isenthalpic cases in Table 3.

Table 3. Heat exchange *TdS* according to chemical, thermal and mechanical paths (Eq. (17)).

***TdS* at equilibrium**	**Isenthalpic**	**Isentropic**
Formation: TS_{vap}	35160	34940
Chemical: *TdS* [μ]	8510	8710
Mechanical: *TdS* [*dP*]	13230	16940
Thermal: *TdS* [*dH*] = apparent heat	–47260	–60550
Total transfer	9646	~ 0

As δQ and dS have the same sign, the entropy production pathways are identified. Thus, the phase change corresponds to a net creation of entropy (*TdS* [formation]). The reduction of the chemical potential by diffusion corresponds to an increase in the entropy of the system (*TdS* [μ]). The loss of pressure is also a source of increase in entropy (*TdS* [*dP*]). Thermal cooling decreases the total entropy. Cooling is the only operation that absorbs entropy (*TdS* [*dH*]), while changing state is the operation that produces the most (see Fig. 5).

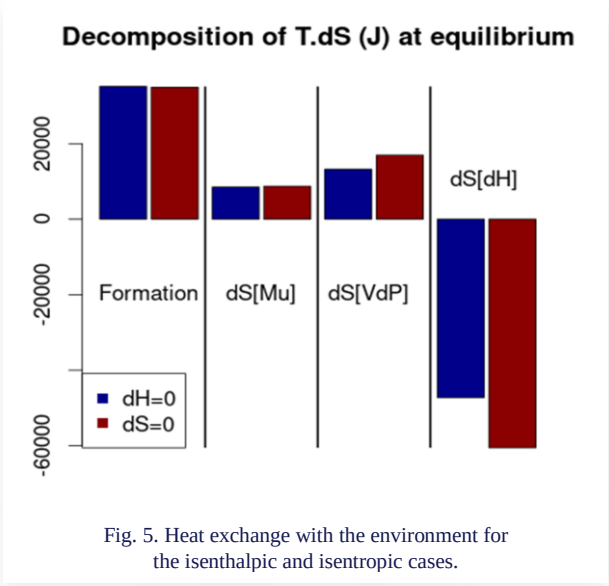

Fig. 5. Heat exchange with the environment for the isenthalpic and isentropic cases.

Apparent heat corresponds to the transfer of latent energy into sensible energy (*TdS* [*dH*]). The term 'apparent heat' is the usual term, although it is here a question of cooling. This energy transfer is internal to the system, but perceptible by measuring its temperature. In the isenthalpic case, this term is more or less equal to the latent energy transfer, i.e. the energy required for modifying the enthalpy of formation due to phase change.

In the isentropic case, there is no exchange with the environment. The case is however irreversible, because irreversible diffusion processes are taken into account in the Gibbs-Duhem equation. This case is truly adiabatic (without any exchange with the environment), even if irreversible. Compared to the isenthalpic case, the energy dissipated in the pressure loss and diffusion is increased. So, the irreversibilities rise in the isentropic case. But the apparent heat increases more, as shown in Fig. 5: at equilibrium, the system is colder because the latent energy transfer is increased. This internal transfer is sufficient to compensate for the energy dissipation. The absence of heat input from the outside prevents any heating of the system.

In the isenthalpic case, heat from the outside (remaining term: 9646 J) corresponds to uncompensated heat; it is not linked to the system temperature and represents 20% of the apparent heat. It is not perceptible by a temperature measurement, but contributes to the reactive blocking. It includes some *PV* energy changes related to pressure drop by cooling and irreversible diffusion as well.

Irreversibilities and cold production both increase in the isentropic case compared to the isenthalpic case. Comparisons to measurements show that real cases are close to the isenthalpic and are not truly adiabatic.

3.5. Efficiency of spray cooling

The isenthalpic equilibrium, described by Eq. (11) with the temperature coming from the isenthalpic Eq. (13), is given by

$$0 = H_{vap} - \left(T_m - \beta_1 x - \beta_2 \frac{x^2}{2}\right) S_{vap} + \\ + R\left(T_m - \beta_1 x - \beta_2 \frac{x^2}{2}\right) \ln\left(\frac{n_v + x}{n_l - x} \frac{kx}{n_g} \frac{T_m - \beta_1 x - \beta_2 \frac{x^2}{2}}{T_m}\right). \quad (18)$$

It is solved for various operating conditions using real data for cooling air with a spray. Measurements were obtained by Surheshkumar et al. [4] for the first series, and by Tissot et al. [5] for the second series. In both papers, operating conditions (T_l, T_g, M_l, M_g, RH) at the wind tunnel inlet are fully given (or retrieved from air volume rate and wet bulb temperature). The atmospheric pressure was not given and we take the standard value in calculations (101 325 Pa).

The standard spray cooling efficiency is given by the ratio between the air temperature decrease between the inlet and the outlet, versus the maximal decrease, given by the difference between wet and dry bulb temperature:

$$\eta = \frac{T_{real} - T_{g,inlet}}{T_{wb,g,inlet} - T_{g,inlet}}. \quad (19)$$

An average temperature at the outlet was computed from operational conditions and Eq. (18). Modelled temperatures are compared with measurements made at the wind tunnel exit in Fig. 6 for the first series and in Fig. 7 for the second one. A perfect efficiency would have been achieved if blue temperatures were aligned with the red ones. In all these experiments, saturation was not reached.

A good agreement was found between the real efficiency of spray and the temperature derived from modelling chemical and thermal equilibrium (Figs. 6 and 7). The evaporation rate is also

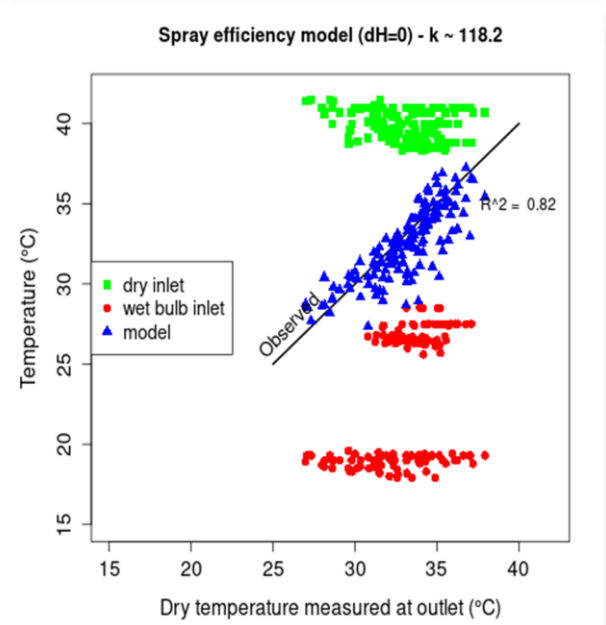

Fig. 6. Temperatures measured by Sureshkumar et al. [4]: dry bulb (green) and wet bulb (red) at the wind tunnel inlet, modelled (blue) and observed (black line) at the wind tunnel outlet. The green-red interval corresponds to the ideal cooling.

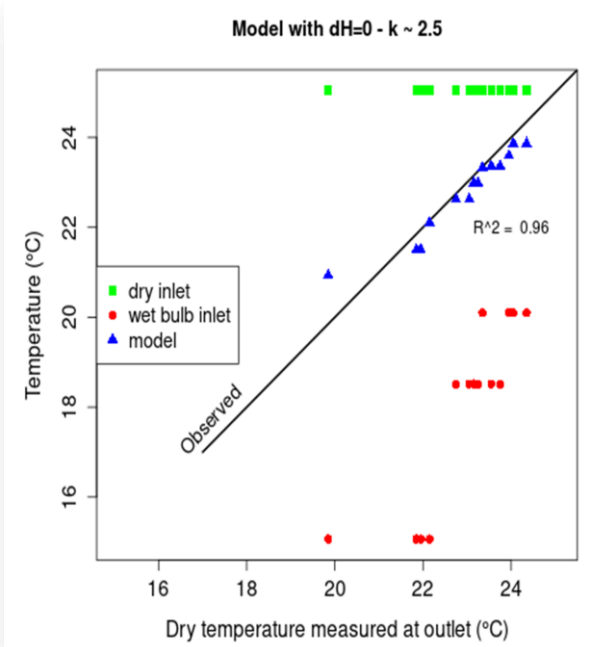

Fig. 7. Temperatures measured by Tissot et al. [5]: dry bulb (green) and wet bulb (red) at the wind tunnel inlet, modelled (blue) and observed (black line) at the wind tunnel outlet.

close to measurements and the temperatures at the outlet were close to an equilibrium. However, the isenthalpic model needs scaling for obtaining such results; the fugacity term was scaled with a scaling factor k.

$$dS_v = -RT \ln \frac{kx}{n_g + x}. \quad (20)$$

The scaling was needed because the liquid content was neglected in writing the entropy of volume change. The volume of vapour starts from small volumes around droplets and should therefore depend on the droplet concentrations. This is the meaning of the scaling factor, which is related to the volume concentration of droplets:

$$k = \frac{n_g + x}{n_t} \left(\frac{n_l - x}{n_l} \frac{\rho_l}{\rho_g} \right)^{\alpha}. \quad (21)$$

Differences between the experiments depend precisely on the droplet concentrations and sizes. The reported sizes are about 10−30 µm in Tissot et al. [5] and bigger in Sureshkumar et al. [4], of about 100 µm to 300 µm. The surface of the liquid was, however, equivalent in the experiment, because Sureshkumar et al. compensated for the small specific surface of droplets by injecting more water. Evaporation of large droplets is more likely related to a droplet size reduction. Due to the high capillary pressure inside the liquid, evaporation reduces droplet numbers rather than the diameters for small droplets [41]. The volume of liquid is expressed by

$$V_l = \frac{(n_l - x)\,\widehat{M}_l}{\rho_l} = \frac{N_d \pi d_d^3}{6}. \quad (22)$$

Reducing the size of droplets (d_d) does not have the same effect on the volume concentration as reducing the number of droplets (N_d). The volumetric concentration depends on whether N_d or d_d varies with x, according to Eq. (22). This changes the exponent α in the scaling factor (Eq. (21)), which is 6/8 for the evolution of d_d [4] and 1/8 for the evolution of N_d [5]. The average value for k (all data of each series) is given in the figures' titles and is related to the hypothesis made on how the volume fraction of droplets decreases with evaporation.

As shown in Fig. 8, heat exchange at the boundaries accounts for more than 20% of the cooling power in the study of Tissot et al. [5], and for approximately 10% in the case of Sureskumar et al. [4]. The relationship between boundary heat and the system follows a linear trend with the temperature gradient for Tissot's measurements, but more discrepancies are observed in Sureskumar's measurements. This can be attributed to the higher water content; the temperature gradients are scattered by the water temperature during mixing. The liquid content also influences the calorific capacities of mixtures. The heat exchange corresponds to the uncompensated heat involved in irreversible processes, such as water vapour diffusion or pressure drop. The more evaporation and efficient cooling, the greater the irreversibility of the processes. Even when cooling is balanced by water evaporation, other energy redistributions are involved in evaporative cooling. These energies prevent the system from reaching the saturated state and govern the effective cooling efficiency.

The model accounts for some of the observed phenomena reported by the authors. The measurements made by Tissot et al. were made at 5 cm and 20 cm downwards the injection point. Measurements were very close in both sections for most of the cases. As the chemical equilibrium was reached, the maximum permissible cooling was achieved under the operational conditions. Hence, the chemical potential explains why evaporation was rather null between sections. Results also indicate that the

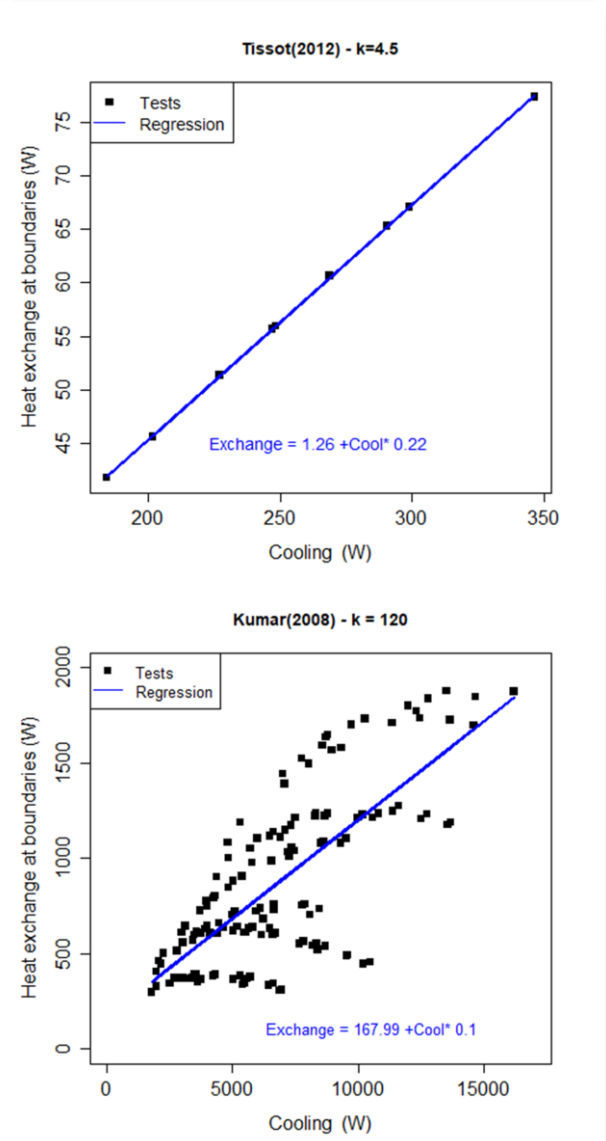

Fig. 8. Heat exchange at the boundaries according to the cooling power related to equilibrium in Tissot et al. [5] experiments (top) and in Sureshkumar et al. [4] experiments (bottom).

equilibrium is rapidly achieved. In half of the data of [4], the injection of water was in the counter-current direction of the air flow. Such an orientation fails to improve cooling efficiency notably, which is mainly limited by the chemical blockage. It may help, however, to get more homogeneous temperatures at the outlet, but was not seen as an explanation factor for improving our estimate.

4. Conclusions and perspectives

By using the Gibbs-Duhem equation to describe the evaporation of liquid water in air, it is possible to study the irreversible processes in the evolution of such a mixture. Four stages are used to distinguish processes and quantify the governing energy pathways of the system, involving mechanical, chemical and thermal energy changes. The Gibbs-Duhem equation allows to study energy redistributions and identify the limiting phenomena when multiple pathways are involved.

With spray cooling, the physicochemical evaporation reaction governs the evolution of the mixture and rules the cooling efficiency. The chemical potential is depleted before the air reaches the adiabatic saturation, due to irreversibilities associated with the diffusion of water vapour in gas: the variation of the volume entropy allows expressing a chemical fugacity and thereby sizes the ending state of the mixture. The chemical potential limits the quantity of spontaneously evaporable water, although vapour diffusion is a process that requires little energy. Other entropic contributions, such as the change of state of water molecules or loss of pressure through cooling, are more important sources of entropy production. Apparent heat (here, apparent cooling) absorbs this production.

In an isentropic transformation, the cooling is maximum and fully compensates for the entropic production, half of which is linked to irreversibilities in the chemical (diffusion, formation) and mechanical (pressure drop) pathways. The transformation takes place without any heat exchange with the outside. In an isenthalpic transformation, the quantity of water evaporated is quite similar, but the cooling is less. Heat is received from the hot surrounding environment and provides an increase of entropy of this system. For such a transformation, the chemical potential also limits the cooling, but the heat received from the environment reduces it. The isenthalpic transformation is not adiabatic, due to the need for this uncompensated heat, which is necessary for the system evolution. An isentropic cooling is more efficient than the isenthalpic cooling and it corresponds to a minimum of entropy. However, entropy production is higher for the isentropic cooling and is compensated by a higher destruction. Both cases do not reach the adiabatic saturation when considering a finite volume.

The isenthalpic equilibrium was applied to real measurements. A scaling was made to account for the volume concentration of droplets in the fugacity model. When scaled, results were found in good agreement with the literature data regarding the spray cooling efficiency. The equilibrium equation gives estimates of efficiencies over a wide range of operating conditions and could help in improving management of spray cooling. The entropic analysis also provides insights about some reported observations and gives an estimate of heat transferred from the surrounding into the system. Surface tension phenomena have to be further described to provide more details about the scaling factor used to correct fugacity. Further experiments, including pressure measurements, are required to assess the ability of the approach to handle with combined pathways, to assess the mechanical energy depletion in such systems.

References

[1] Meng, X., Meng, L., Gao, Y., & Li, H. (2022). A comprehensive review on the spray cooling system employed to improve the summer thermal environment: Application efficiency, impact factors, and performance improvement. *Building and Environment*, 217, 109065. doi: 10.1016/j.buildenv.2022.109065

[2] Kachhwaha, S.S., Dhar, P.L., & Kale, S.R. (1998). Experimental studies and numerical simulation of evaporative cooling of air with a water spray — I. Horizontal parallel flow. *International Journal of Heat and Mass Transfer*, 41(2), 447–464. doi: 10.1016/S0017-9310(97)00133-6

[3] Hamlin, S., Hunt, R., & Tassou, S.A. (1998). Enhancing the performance of evaporative spray cooling in air cycle refrigeration and air conditioning technology. *Applied Thermal Engineering*, 18(11), 1139–1148. doi: 10.1016/S1359-4311(98)00028-3

[4] Sureshkumar, R., Kale, S.R., & Dhar, P.L. (2008). Heat and mass transfer processes between a water spray and ambient air – I. Experimental data. *Applied Thermal Engineering*, 28(5-6), 349–360, doi: 10.1016/j.applthermaleng.2007.09.010

[5] Tissot, J., Boulet, P., Labergue, A., Castanet, G., Trinquet, F., & Fournaison, L. (2012). Experimental study on air cooling by spray in the upstream flow of a heat exchanger. *International Journal of Thermal Sciences*, 60, 23–21, doi: 10.1016/j.ijthermalsci.2012. 06.005

[6] Zheng, K., Ichinose, M., & Wong, N.H. (2018). Parametric study on the cooling effects from dry mists in a controlled environment. *Building and Environment*, 141, 61–70. doi: 10.1016/j.buildenv. 2018.05.053

[7] Sun, Y., Alkhedhair, A.M., Guan, Z., & Hooman, K. (2018). Numerical and experimental study on the spray characteristics of full-cone pressure swirl atomizers. *Energy*, 160, 678-692. doi: 10.1016/ j.energy.2018.07.060

[8] Caliskan, H., Hepbasli, A., Dincer, I., & Maisotsenko, V. (2011). Thermodynamic performance assessment of a novel air cooling cycle: Maisotsenko cycle. *International Journal of Refrigeration*, 34(4), 980−990. doi: 10.1016/j.ijrefrig.2011.02.001

[9] Zhan, C., Duan, Z., Zhao, X., Smith, S., Jin, H., & Riffat, S. (2011). Comparative study of the performance of the M-cycle counter-flow and cross-flow heat exchangers for indirect evaporative cooling – Paving the path toward sustainable cooling of buildings. *Energy*, 36(12), 6790−6805. doi: 10.1016/j.energy. 2011.10.019

[10] Jia, C., Sun, D., Hu, X., & Jing, C. (2023). Optimization of the performance of M-Cycle indirect evaporative cooling via thermodynamic approach. *Journal of Asian Architecture and Building Engineering*, 22(6), 3612−3626. doi: 10.1080/13467581.2023. 2183774

[11] Yang, H., Shi, W., Chen, Y., & Min, Y. (2021). Research development of indirect evaporative cooling technology: An updated review. *Renewable and Sustainable Energy Reviews*, 145, 111082. doi: 10.1016/j.rser.2021.111082

[12] Wang, T., Sheng, C., & Agwu Nnanna, A.G. (2014). Experimental investigation of air conditioning system using evaporative cooling condenser. *Energy and Buildings*, 81, 435−443. doi: 10.1016/ j.enbuild.2014.06.047

[13] Wen, M.-Y., Ho, C.-Y., Jang, K.-J., & Yeh, C.-H. (2014). Experimental study on the evaporative cooling of an air-cooled condenser with humidifying air. *Heat and Mass Transfer*, 50, 225–233. doi: 10.1007/s00231-013-1243-7

[14] Heidarinejad, G. As'adi Moghaddam, M.R., & Pasdarshahri, H. (2019). Enhancing COP of an air-cooled chiller with integrating a water mist system to its condenser: Investigating the effect of spray nozzle orientation. *International Journal of Thermal Sciences*, 137, 508−525. doi: 10.1016/j.ijthermalsci.2018.12.013

[15] Yang, H., Rong, L., Liu, X., Liu, L., Fan, M., & Pei, N. (2020). Experimental research on spray evaporative cooling system applied to air-cooled chiller condenser. *Energy Reports*, 6, 906−913. doi: 10.1016/j.egyr.2020.04.001

[16] Smrekar, J., Oman, J., & Širok, B. (2006). Improving the efficiency of natural draft cooling towers. *Energy Conversion and Management*, 47(9-10), 1086−1100. doi: 10.1016/j.enconman. 2005.07.012

[17] Muangnoi, T., Asvapoositkul, W., & Wongwises, S. (2008). Effects of inlet relative humidity and inlet temperature on the performance of counterflow wet cooling tower based on exergy analysis. *Energy Conversion and Management*, 49(10), 2795− 2800. doi: 10.1016/ j.enconman.2008.03.019

[18] Alkhedhair, A., Guan, Z., Jahn, I., Gurgenci, H., & He, S. (2015). Water spray for pre-cooling of inlet air for Natural Draft Dry Cooling Towers – Experimental study. *International Journal of Thermal Sciences*, 90, 70−78. doi: 10.1016/j.ijthermalsci. 2014. 11.029

[19] Kim, M.-H., & Jeong, J.-W. (2013). Cooling performance of a 100% outdoor air system integrated with indirect and direct evaporative coolers. *Energy*, 245−257. doi: 10.1016/j.energy. 2013.02.008

[20] Zunaid, M., Murtaza, Q., & Gautam, S. (2017). Energy and performance analysis of multi droplets shower cooling tower at different inlet water temperature for air cooling application. *Applied Thermal Engineering*, 121, 1070−1079. doi: 10.1016/j.applthermaleng.2017.04.157

[21] Tejero-González, A., & Franco-Salas, A. (2021). Optimal operation of evaporative cooling pads: A review. *Renewable and Sustainable Energy Reviews*, 151. 111632. doi: 10.1016/j.rser.2021. 111632

[22] Lee, Y.-C., Chen, K.-Y., Yan, W.-M., Shih,Y.-C., & Chao, C.-Y. (2023). Evaporative cooling method to improve energy management of overhead downward flow-type data center. *Case Studies in Thermal Engineering*, 45, 102998. doi: 10.1016/j.csite.2023. 102998

[23] Mi, R., Bai, X., Xu, X., & Ren, F. (2023). Energy performance evaluation in a data center with water-side free cooling. *Energy and Buildings*, 295, 113278. doi:10.1016/j.enbuild.2023.113278

[24] Elahi, S.H., & Farhani, S.D. (2021). Increasing evaporative cooler efficiency by controlling water pump run and off times. *International Communications in Heat and Mass Transfer*, 127, 05525. doi: 10.1016/j.icheatmasstransfer.2021.105525

[25] Feidt, M. (2013). *Thermodynamique optimale en dimensions physiques finies*. In Collection Thermique, par Denis Lavoisier. Lavoisier – Hermes Science Publications.

[26] Dumouchel, C. (2009). The Maximum Entropy Formalism and the Prediction of Liquid Spray Drop-Size Distribution. *Entropy*, 11(4), 713–747. doi: 10.3390/e11040713

[27] Le Moyne, L., Freire, V. & Queiros Conde, D. (2008). Fractal dimension and scale entropy applications in a spray. *Chaos, Solitons & Fractals*, 38(3), 696−704, doi: 10.1016/j.chaos.2007. 01.004

[28] Bejan, A. (2016). *Advanced Engineering Thermodynamics.* John Wiley & Sons, Inc.

[29] Pauluis, O. M. (2004). Chapter 7: Water vapor and entropy production in the earth's atmosphere. In , *Non-equilibrium thermodynamics and the production of entropy: Life, Earth and Beyond* (A. Kelidon, R. D. Lorenz, Eds.). Springer-Verlag.

[30] Duane, G.S. & Curry, J.A. (1997). Entropy of a convecting water-air system and the interpretation of cloud morphogenesis. *Quarterly Journal of the Royal Meteorological Society*, 123 (539), 605−629. doi: 10.1002/qj.49712353905

[31] Barton, N.G. (2008). An evaporation heat engine and condensation heat pump. *Anziam Journal*, 49(4), 503−524. doi: 10.1017/ S1446181108000035

[32] Chengqin, R., Nianping, L. & Guangfa, T. (2002). Principles of exergy analysis in HVAC and evaluation of evaporative cooling schemes. *Building and Environment*, 37(11), 1045−1055. doi: 10.1016/S0360-1323(01)00104-4

[33] Ratlamwala, T.A.H. & Dincer, I. (2013). Efficiency assessment of key psychometric processes. *International Journal of Refrigeration*, 36(3), 1142−1153, doi: 10.1016/j.ijrefrig.2012.10.038

[34] Santos, J.C., Barros, G.D.T., Gurgel, J.M. & Marcondes, F. (2013). Energy and exergy analysis applied to the evaporative cooling process in air washers. *International Journal of Refrigeration*, 36(3), 1154−1161. doi: 10.1016/j.ijrefrig.2012.12.012

[35] Wang, L., Zhan, L.C., Zhang, J. & Zhao, X. (2019). Optimization of the counter-flow heat and mass exchanger for M-cycle indirect evaporative cooling assisted with entropy analysis. *Energy*, 171, 1205−1216. doi:10.1016/j.energy.2019.01.099.

[36] Manjunath, K. & Kaushik, S.C. (2014). Second law thermodynamic study of heat exchangers: A review. *Renewable and Sustainable Energy Reviews*, 40, 348−375. doi: 10.1016/j.rser.2014.07.186

[37] Niven, R.K. & Noack, B.R. (2013). Control volume analysis, entropy balance and the entropy production in flow systems. In *Beyond the Second Law: Entropy Production and Non-Equilibrium Systems* (R.C. Dewar, C. Lineweaver, R.K. Niven., K. Regenauer-Lieb, Eds.) (pp. 129−162). Springer-Verlag.

[38] Feidt, M. (2016). *Thermodynamique et optimisation énergétique des systèmes et procédés*. Hors collection, Lavoisier.

[39] Farmahini-Farahani, M., Delfani, S. & Esmaeelian, J. (2012). Exergy analysis of evaporative cooling to select the optimum system in diverse climates. *Energy*, 40(1), 250−257, doi: 10.1016/j.energy.2012.01.075

[40] Lacour, S.O.L., Diango, K.A. & Feidt, M. (2022). Entropy analysis in spray cooling for dosing water injection. *Entropie: thermodynamique – énergie – environnement – économie*, 3(1) (in French). doi: 10.21494/ISTE.OP.2022.0829

[41] Lefebvre, A. (1988). *Atomization and Sprays* (1st ed.). CRC Press. doi: 10.1201/9781482227857